

Short Communication

Electrolytic Recovery of Aluminum from 1-Butyl-3-methylimidazolium Bis(trifluoromethanesulfonyl)imide Ionic Liquid Containing AlCl_3

Yong Zheng^{1,*}, Qian Wang², Yongjun Zheng¹, Zhen Wang¹, Dayong Tian¹

¹ College of Chemical and Environmental Engineering, Anyang Institute of Technology, Anyang 455000, P. R. China

² State Key Laboratory of Multiphase Complex Systems, Institute of Process Engineering, Chinese Academy of Sciences, Beijing 100190, P. R. China

*E-mail: yzheng83@126.com

Received: 2 June 2022 / Accepted: 17 July 2022 / Published: 7 August 2022

Electrolytic recovery of pure aluminum is a conventional method for the recycling of waste aluminum alloys, which is very important to economic development and environmental protection. However, the conventional electrolytic recovery process suffers from several inherent problems, which restricts the further development of this technology. In this study, an air- and moisture-stable 1-butyl-3-methylimidazolium bis(trifluoromethanesulfonyl)imide ionic liquid was applied in the dissolution of aluminum chloride. The upper phase of the resulting mixture was used as a low-temperature electrolyte in the electrolytic recovery of pure aluminum. The results of cyclic voltammetry and linear sweep voltammetry showed that aluminum could be electrodeposited from the electrolyte and that the main impurity elements of the aluminum alloy could also be stripped off by the electrolytic method. Based on these measurements, the electrolytic recovery process was conducted at 0.2–0.6 V and 303.2–373.2 K. Scanning electron microscope micrographs showed that smooth, compact and well-adherent deposits were obtained at 0.4 V from 303.2 to 323.2 K. In this situation, the preferred crystallographic orientation of these deposits was the (200) plane. Meanwhile, the mass content of aluminum in all deposits was higher than 99.6% according to the purity characterization. This study may be useful for the further application of ionic liquids in the low-temperature recycling of waste aluminum alloys.

Keywords: aluminum; electrolytic recovery; ionic liquid; aluminum alloy

1. INTRODUCTION

Aluminum is the most plentiful metal element in the Earth's crust. The traditional production of aluminum is generally conducted by the famous Hall-Héroult electrolytic process, which finally yields commercial primary aluminum with 99.5–99.8% purity [1-3]. In 2021, the global production and

consumption of primary aluminum were approximately 67 and 69 million tons, respectively. Meanwhile, the widespread usage of aluminum leads to a large amount of waste aluminum alloys worldwide. From the perspective of economic development and environmental protection, more efforts should be made to promote the recycling of waste aluminum alloys [4,5].

Electrolytic recovery of pure aluminum is a conventional method for the recycling of waste aluminum alloys, which is often performed in inorganic molten salts with temperatures in excess of 700 °C [6-9]. For example, the so-called three-layer electrolytic method is conducted in a solution of cryolite above the melting point of aluminum [7]. However, this method suffers from several inherent problems, such as excessive energy consumption and complex operation [8,9]. Therefore, it is necessary to develop more environmentally friendly and high-efficiency technologies.

Ionic liquids (ILs) have been widely used as green solvents and electrolytes owing to their excellent physicochemical properties [10-12]. From prior work, aluminum can be electrodeposited from the ILs below 100 °C with remarkable progress achieved in this area over the past decades [13-15]. On this basis, the successful application of ILs in aluminum electrodeposition paves the way for the low-temperature recovery of pure aluminum from aluminum alloys. The corresponding energy consumption and cell voltage are less than 3 kWh/kg and 1 V, respectively [16,17]. Until now, the most studied ILs have been those containing Lewis acidic chloroaluminate anions [18-20]. Compared with traditional methods, the electrolytic recovery of aluminum in ILs is more energy-efficient and environmentally friendly [21]. However, research on the electrochemical mechanism and experimental conditions remains limited. Meanwhile, the moisture sensitivity of chloroaluminate ILs restricts the further development of this technology in industry [22,23]. In this situation, air- and moisture-stable bis(trifluoromethanesulfonyl)imide-based ILs have attracted increasing attention as novel media for the low-temperature electrodeposition of aluminum worldwide [24-26]. Consequently, we investigated the application of these ILs in the electrolytic recovery of pure aluminum from aluminum alloys.

In this work, 1-butyl-3-methylimidazolium bis(trifluoromethanesulfonyl)imide ([Bmim][NTf₂]) IL was used as an air- and moisture-stable solvent. The addition of aluminum chloride into the IL with a molar ratio of 2:1 yielded the desired electrolyte, namely, [Bmim][NTf₂]-2AlCl₃. Then, the upper layer of [Bmim][NTf₂]-2AlCl₃ was used in the electrolytic recovery of pure aluminum from aluminum alloy [24,26]. Based on voltammetry measurements, the electrolytic recovery process was performed at different temperatures and potentials. The surface morphology, purity and crystallographic orientation of pure aluminum were characterized. Finally, the experimental results were analyzed and discussed.

2. EXPERIMENTAL PROCEDURE

2.1 Chemicals

[Bmim][NTf₂] was obtained from Linzhou Keneng Material Technology Co., Ltd. Anhydrous aluminum chloride, alumina powder, absolute ethanol, acetone, hydrochloric acid and sulfuric acid were purchased from Sinopharm Chemical Reagent Co., Ltd. and were of analytic grade. Aluminum, zinc, copper, iron and silicon plates were provided by Shanghai Aladdin Biochemical Technology Co.,

Ltd. and Sinopharm Chemical Reagent Co., Ltd., with a mass fraction purity higher than 0.999. Aluminum alloy was obtained from Beijing Nonferrous Metals & Rare Earth Research Institute, which was used as a model of waste aluminum alloy and consisted of approximately 5.2 wt.% copper, 0.9 wt.% iron, 0.6 wt.% silicon, 0.5 wt.% zinc and 0.3 wt.% other impurities. Prior to use, [Bmim][NTf₂] was extracted with ultrapure water, distilled by evaporation and dried under vacuum at 353 K for 24 h.

2.2 Preparation of [Bmim][NTf₂]-2AlCl₃

0.2 mole of anhydrous aluminum chloride was slowly added to 0.1 mole of [Bmim][NTf₂] in an inert atmosphere glove box (LABstar, Mbraun) at room temperature, where the mass contents of oxygen and water were each less than 1 mg/kg. Then, the mixture was stirred at 353.2 K on a magnetic stirrer (RCT digital, IKA) until a transparent solution of [Bmim][NTf₂]-2AlCl₃ was formed. After the solution was cooled to ambient temperature, the upper phase was separated and used as a low-temperature electrolyte for the recovery of pure aluminum. The molar concentration of aluminum chloride in [Bmim][NTf₂]-2AlCl₃ was approximately 5 mol/kg according to the literature [24-26].

2.3 Characterization of ILs

The final mass fraction purity of [Bmim][NTf₂] was higher than 0.995 according to the measurements of NMR (av-400, Bruker), triple quadrupole LC/MS (G6420, Agilent) and IR spectra (iS10, Nicolet). The upper phase of [Bmim][NTf₂]-2AlCl₃ was characterized by ¹H NMR, ¹³C NMR and ²⁷Al NMR. Meanwhile, the water content of the ILs was determined to be less than 50 mg/kg based on the Karl Fisher method (751 GPD Titrino, Metrohm).

2.4 Electrochemical experiments

All electrochemical experiments were performed in a glove box with an inert atmosphere. The experimental temperature was controlled using a magnetic stirrer equipped with an electronic contact thermometer (ETS-D6, IKA) with an accuracy of ±0.2 K. The atmospheric pressure was 101.3 kPa, which was controlled by a programmable logic controller. A three-electrode cell was used in these experiments, and the cell was regulated with an electrochemical station (CHI660E, Chenhua). In all measurements, the counter and reference electrodes were platinum plate (99.99%, Ida) and aluminum wire (99.99%, Ida), respectively. In the cyclic voltammetry and electrolytic recovery experiments, platinum and aluminum alloy plates were applied as working electrodes, respectively. To investigate the electrochemical behavior of alloy elements, linear sweep voltammetry experiments were performed, and the working electrodes included aluminum, zinc, copper, iron and silicon plates. The potential scan rate in all voltammetry measurements was 50 mV/s. Before use, all electrodes were polished with alumina, treated with a mixture of sulfuric and hydrochloric acids, cleaned with ultrapure water and absolute ethanol and finally dried in cool air. The recovery of pure aluminum was conducted using a potentiostatic electrolysis method at 0.2–0.6 V and 303.2–373.2 K for 1 h. The resulting aluminum

deposits were washed with absolute ethanol and acetone, and dried under an inert atmosphere.

2.5 Characterization of aluminum deposits

The purity of aluminum deposits was determined with an energy-dispersive spectrometer (Inca, Oxford), inductively-coupled plasma optical emission spectroscopy (5100, Agilent) and aluminum portable photometer (HI96712, Hana). The surface morphology and X-ray diffraction (XRD) patterns of aluminum deposits were characterized using scanning electron microscopy (SEM) (JSM-6700F, JEOL) and X-ray diffraction (D8 Advance, Bruker), respectively.

3. RESULTS AND DISCUSSION

3.1 Cyclic voltammetry

Figure 1 shows the cyclic voltammograms that were obtained on a platinum electrode in the upper phase of [Bmim][NTf₂]-2AlCl₃ at different temperatures. All curves exhibit a pair of oxidation and reduction peaks. The reduction peaks in the negative current region are ascribed to the electrodeposition of aluminum, while the oxidation peaks in the positive current region mainly result from the stripping of aluminum [27,28]. It is apparent that aluminum could be electrodeposited from the IL and that the reaction process is reversible. As the temperature increases from 303.2 to 373.2 K, the initial reduction potential of aluminum increases slightly. A similar trend is also observed in the absolute current values for the reduction and oxidation peaks. This result reveals that Al(III) is prone to reduction and that more aluminum deposits can be obtained at the same potential with increasing temperature. This phenomenon is probably attributed to the enhanced rate of ion and charge transfer.

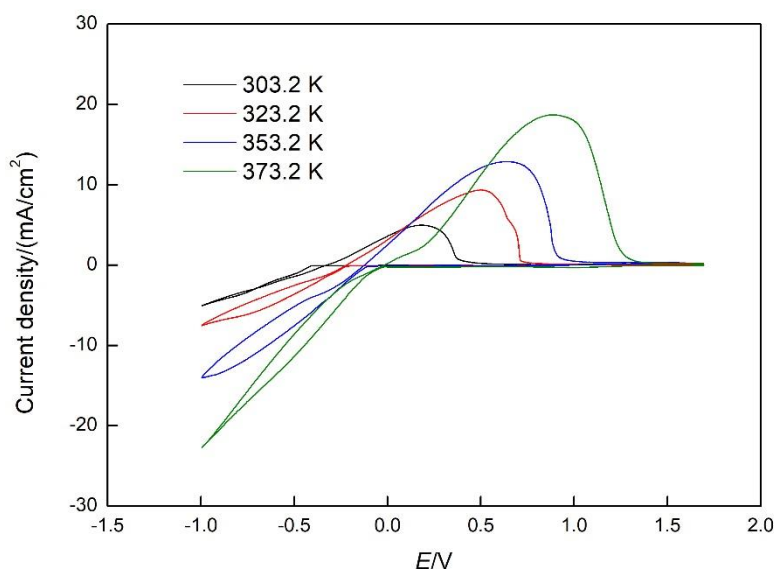
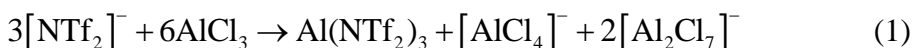


Figure 1. Cyclic voltammograms obtained on a platinum electrode in the upper phase of [Bmim][NTf₂]-2AlCl₃ at different temperatures. The potential scan rate was 50 mV/s.

Previous studies revealed that the electroactive species are expected to be $[\text{AlCl}_3(\text{NTf}_2)]^-$ or $[\text{AlCl}_2(\text{NTf}_2)_2]^-$ for aluminum deposition in $[\text{cation}][\text{NTf}_2]-\text{AlCl}_3$ ILs when the mole fraction of AlCl_3 is less than 0.5 [29,30]. In this work, ^1H NMR, ^{13}C NMR and ^{27}Al NMR were measured to investigate the speciation of aluminum in the IL. However, the results of these measurements show that no NTf_2 -based ions are present in the upper phase of $[\text{Bmim}][\text{NTf}_2]-2\text{AlCl}_3$ when the mole fraction of AlCl_3 is 0.67. In contrast, the active species responsible for aluminum electrodeposition is the $[\text{Al}_2\text{Cl}_7]^-$ anion, which is consistent with the experimental and theoretical findings reported in the literature and our previous work [24,31,32]. The reaction between $[\text{NTf}_2]^-$ and AlCl_3 can be illustrated with the following formula:



3.2 Linear sweep voltammetry

To achieve the electrolytic recovery of pure aluminum from aluminum alloy, it is necessary to study the electrochemical behavior of corresponding elements. Therefore, linear sweep voltammograms were recorded on different working electrodes, which were composed of the corresponding elements in the upper phase of $[\text{Bmim}][\text{NTf}_2]-2\text{AlCl}_3$.

As Figure 2 shows, the initial oxidation potentials of aluminum, zinc, iron and copper are approximately 0.2, 0.6, 0.8 and 0.95 V, respectively. However, no significant oxidation reaction is observed for silicon in the linear sweep voltammograms. It is obvious that the initial oxidation potentials of these elements are quite different from each other. Therefore, all impurity elements, including zinc, iron, copper and silicon can be separated from aluminum alloy by the electrolytic method [16]. The various electrochemical behaviors of these elements facilitate the electrolytic process.

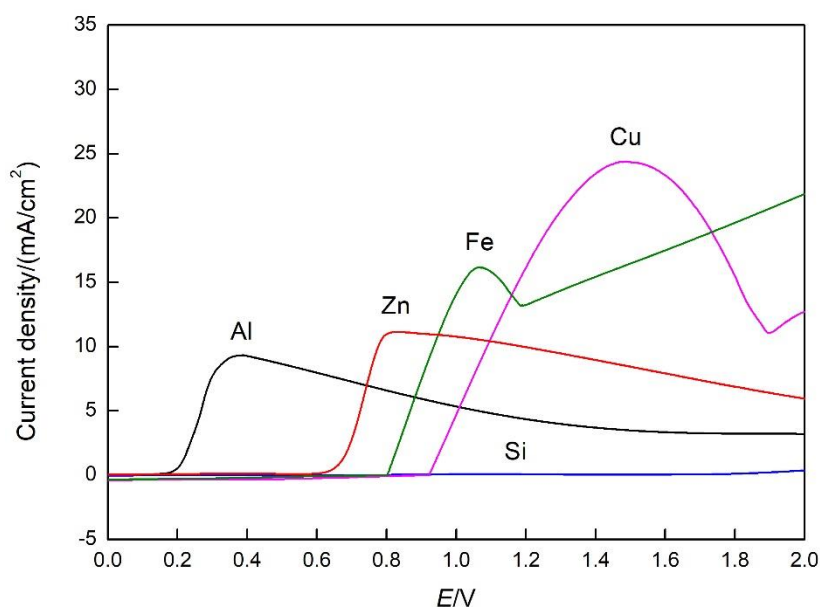


Figure 2. Linear sweep voltammograms obtained on different working electrodes in the upper phase of $[\text{Bmim}][\text{NTf}_2]-2\text{AlCl}_3$ at 303.2 K. The potential scan rate was 50 mV/s.

Figure 2 also shows that the oxidation current of these elements first increases and then reaches a maximum with an increase in the applied potential. Then, the decrease in current mainly results from the electrochemical passivation of these elements at higher potentials. Therefore, utilizing a proper potential is very important for the electrolytic recovery of aluminum.

In conclusion, the results of cyclic and linear sweep voltammetry confirm that aluminum can be electrodeposited from the IL and that the main impurity elements can be separated from the aluminum alloy by the electrolytic method. Based on the curves in the linear sweep voltammograms, it can be inferred that the optimal potential for the electrolytic recovery of aluminum is between 0.2 and 0.6 V. Therefore, the potentiostatic electrolysis method was utilized in this work to conduct the electrolytic recovery process.

3.3 Electrolytic recovery of pure aluminum

On the basis of voltammogram measurements, the subsequent electrolytic process was carried out by the potentiostatic electrolysis method at 0.2–0.6 V and 303.2–373.2 K. Thus, the influence of the experimental potential and temperature on the electrolytic recovery of pure aluminum from aluminum alloy was investigated and is discussed in detail.

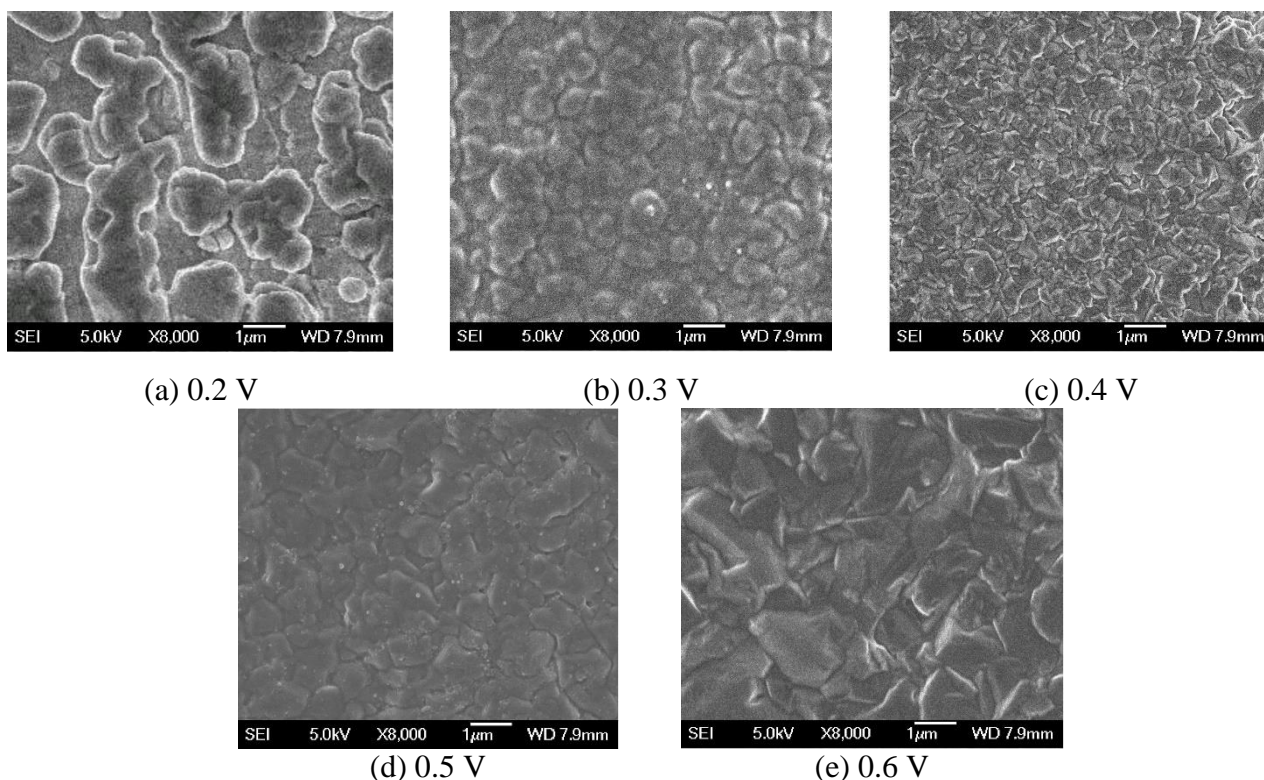


Figure 3. SEM micrographs of aluminum deposits obtained from the electrolytic recovery process at 303.2 K and different potentials.

The experimental potential has a remarkable effect on the surface morphology and purity of aluminum deposits obtained from the electrolytic recovery process. As Figure 3 illustrates, the average

grain size of the deposits decreases when the experimental potential increases from 0.2 to 0.4 V at 303.2 K. However, the average grain size begins to increase as the applied potential rises in the range of 0.4–0.6 V. This indicates that more aluminum nuclei could be formed when the oxidation current density of the aluminum alloy reaches a maximum at 0.4 V [32,33]. In contrast, the decrease in oxidation current density results in fewer aluminum nuclei at other applied potentials. As a result, smooth and compact aluminum deposits are obtained at 0.4 V and 303.2 K. These findings support the hypothesis that the process of aluminum electrodeposition in ILs can be sufficiently described by the three-dimensional instantaneous nucleation/growth model [32-34].

The influence of experimental temperature on aluminum deposits was also studied and analyzed by using SEM micrographs. As Figures 4 and 3c show, the grain size of the aluminum crystals increases quickly when the temperature increases from 303.2 to 373.2 K. This result suggests that the growth rate and reduction current density of aluminum are enhanced with increasing temperature. Consequently, more aluminum crystals are finally deposited and overlap on the surface of the substrate, resulting in many large aluminum deposits. Under such circumstances, the deposits obtained at higher temperatures display a less compact and poorly adherent surface morphology. In contrast, smooth and well-adherent deposits could be obtained at 0.4 V from 303.2 to 323.2 K. Therefore, it is obvious that the experimental temperature plays an important role in the electrolytic recovery of pure aluminum.

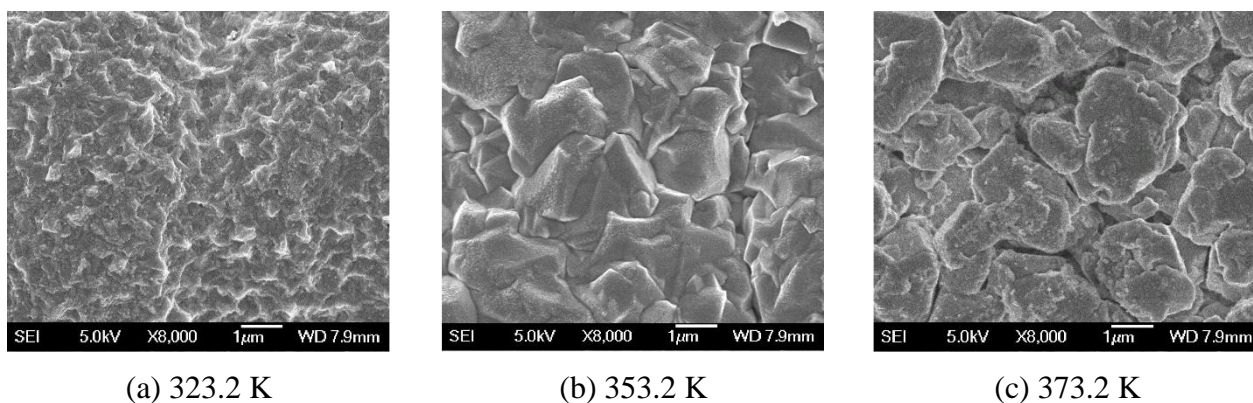


Figure 4. SEM micrographs of aluminum deposits obtained from the electrolytic recovery process at 0.4 V and different temperatures.

The purity of the aluminum obtained in this work was also characterized. It is confirmed that the electrolytic recovery process finally yields a high-purity product with a mass content of aluminum higher than 99.6%. For example, the purity of aluminum deposits obtained at 303.2 K and 0.4 V is more than 99.9%. As Figure 5 shows, no impurity peaks are observed in the energy-dispersive spectrum. This indicates that the main impurity elements of the aluminum alloy could be effectively stripped off in the upper phase of [Bmim][NTf₂]-2AlCl₃ under the studied experimental conditions. Meanwhile, the uniform and compact growth of aluminum on the substrate is beneficial to the electrolytic process by protecting the deposits from further oxidation. Thus, it is proper to state that the optimum potential and temperature ranges for the electrolytic recovery of pure aluminum are 0.4 V

and 303.2–323.2 K, respectively.

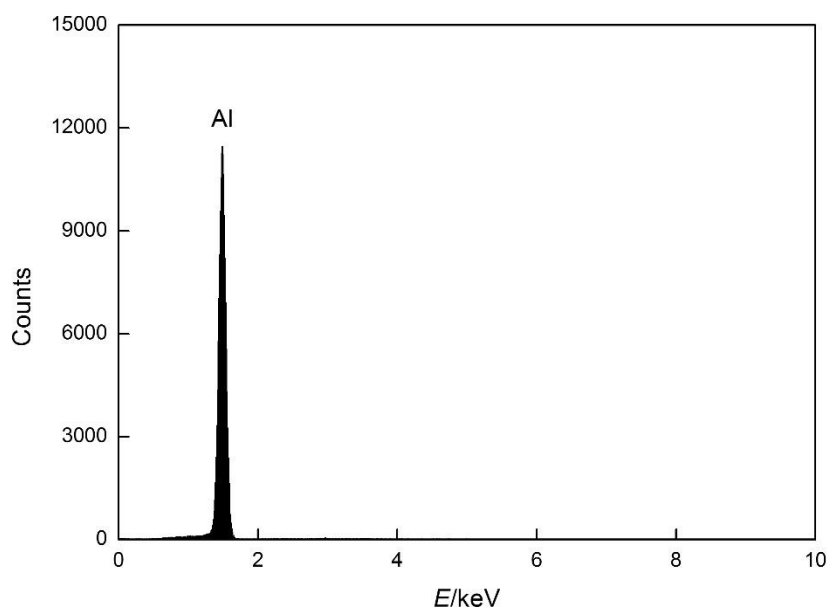


Figure 5. Energy-dispersive spectrum of aluminum deposits obtained from the electrolytic recovery process at 303.2 K and 0.4 V.

The crystal growth and crystallographic orientations of aluminum were further investigated by XRD measurements in this work. Experimental results confirm that all deposits display the classic crystallographic orientations of aluminum reported in JCPDS cards [34,35]. Meanwhile, there are no impurity peaks in these XRD patterns. Consequently, the main chemical composition of these deposits was also determined to be aluminum by XRD measurements. This shows that the crystal patterns of aluminum are highly influenced by the applied potential and experimental temperature. When the deposits exhibit a rough and less compact surface, the corresponding preferred crystallographic orientation is the (111) plane. For example, the deposits obtained at 353.2–373.2 K and 0.5–0.6 V display a preferred crystallographic orientation of the (111) plane. As Figure 6 shows, the preferred growth of aluminum on the substrate shifts to the (200) plane as the surface morphology of deposits becomes smoother and denser at 303.2 K and 0.4 V. Therefore, these results also indicate that the growth process of aluminum is very sensitive to the experimental temperature and applied potential. The crystal structure and surface morphology of aluminum deposits are closely related in the electrolytic process. Similar conclusions have also been obtained in our previous work and literature [36,37]. It can be concluded that the crystal growth of aluminum is not only important to the surface morphology of deposits but also vital to the purity of the aluminum product obtained by the electrolytic recovery process.

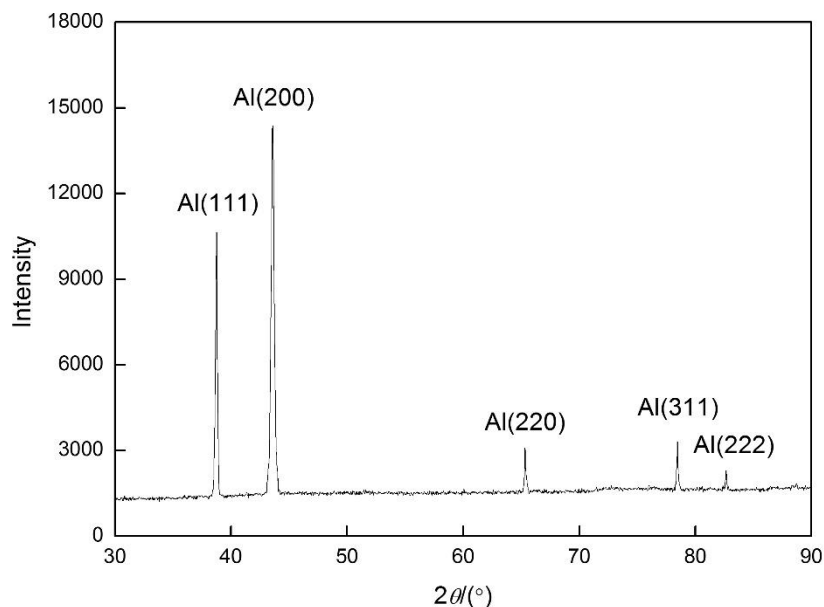


Figure 6. XRD pattern of aluminum deposits obtained from the electrolytic recovery process at 303.2 K and 0.4 V.

4. CONCLUSIONS

In this work, [Bmim][NTf₂]-2AlCl₃ was prepared by the addition of anhydrous aluminum chloride into an air- and moisture-stable [Bmim][NTf₂] IL with a molar ratio of 2:1. Then, the upper phase of the resulting mixture was separated and used as a novel electrolyte for the low-temperature electrolytic recovery of pure aluminum from aluminum alloy. The results of cyclic voltammograms showed that aluminum could be electrodeposited from the electrolyte, and that the reaction process was reversible. The active species responsible for aluminum electrodeposition was determined to be the [Al₂Cl₇]⁻ anion, and the reaction formula between [NTf₂]⁻ and AlCl₃ was also proposed. Meanwhile, linear sweep voltammetry measurement confirmed that all main impurity elements, including zinc, iron, copper and silicon could be effectively separated from the aluminum alloy by the electrolytic method. On the basis of SEM micrographs, smooth, compact and well-adherent aluminum deposits were obtained at 0.4 V from 303.2 to 323.2 K, and the corresponding purity was higher than 99.6%. All deposits displayed the classic crystallographic orientations of aluminum reported in JCPDS cards. The preferred crystallographic orientation of aluminum was the (200) plane when the surface morphology of deposits was smoother and denser. Hence, the optimum potential and temperatures for electrolytic recovery of pure aluminum were 0.4 V and 303.2–323.2 K, respectively. It is expected that this study may be useful for the further application of ILs in the recycling of waste aluminum alloys.

ACKNOWLEDGEMENTS

This work is financially supported by the National Natural Science Foundation of China (No. 21406002, 22178360), the Program for Young Key Teachers in Henan Province (No. 2017GGJS175) and the Scientific Research Foundation of Anyang Institute of Technology (No. YPY2020005).

References

1. M. F. Fini, G. Soucy, M. Désilets, D. Lombard, P. Pelletier and R. Paulus, *Miner. Eng.*, 156 (2020) 106527
2. S. J. Lindsay and B. J. Welch, *JOM*, 73 (2021) 1196
3. L. Barelli, M. Baumann, G. Bidini, P. A. Ottaviano, R. V. Schneider, S. Passerini and L. Trombetti, *Energy Technol.*, 8 (2020) 2000233
4. S. Huan, Y. Wang, J. Peng, Y. Di, B. Li and L. Zhang, *Miner. Eng.*, 154 (2020) 106386
5. S. Capuzzi and G. Timelli, *Metals*, 8 (2018) 249
6. M. Zhang, V. Kamavaram and R. G. Reddy, *JOM*, 55 (2003) 54
7. F. Allard, M. Désilets and A. Blais, *Thermochim. Acta*, 671 (2019) 89
8. A. Yasinskiy, S. K. Padamata, I. Moiseenko, S. Stopic, D. Feldhaus, B. Friedrich and P. Polyakov, *Metals*, 11 (2021) 1053
9. D. Wang, X. Zhong, F. Liu and Z. Shi, *Int. J. Electrochem. Sci.*, 14 (2019) 9482
10. C. F. J. Francis, I. L. Kyratzis and A. S. Best, *Adv. Mater.*, 32 (2020) 1904205
11. S. K. Singh and A. W. Savoy, *J. Mol. Liq.*, 297 (2020) 112038
12. D. Bedrov, J. P. Piquemal, O. Borodin, A. D. MacKerell, B. Boux and C. Schröder, *Chem. Rev.*, 119 (2019) 7940
13. K. K. Maniam and S. Paul, *Coatings*, 11 (2021) 80
14. H. Matsushima, H. Takahashi, T. Suzuki, M. Ueda and I. Mogi, *Electrochem. Commun.*, 115 (2020) 106733
15. M. Li and Y. Li, *Int. J. Electrochem. Sci.*, 15 (2020) 8498
16. S. Z. E. Abedin, *J. Solid State Electrochem.*, 16 (2012) 775
17. D. Pradhan and R. G. Reddy, *Metall. Mater. Trans. B*, 43B (2012) 519
18. S. Wang, Q. Pei, C. Xu, Y. Hua, Q. Zhang, Y. Li, X. Ren and J. Ru, *J. Electrochem. Soc.*, 168 (2021) 012502
19. V. A. Eltermanm, P. Y. Shevelin, L. A. Yolshina and A. V. Borozdin, *Electrochim. Acta*, 389 (2021) 138715
20. Q. Wang, Q. Zhang, X. Lu and S. Zhang, *Ionics*, 23 (2017) 2449
21. Y. Wang, R. G. Reddy and R. Wang, *J. Clean Prod.*, 287 (2021) 125043
22. T. Cosby, D. P. Durkin, R. A. Mantz and P. C. Trulove, *ECS Trans.*, 98 (2020) 117
23. X. Zhang, R. Zhang, H. Liu, X. Meng, C. Xu, Z. Liu and P. A. A. Klusener, *Ind. Eng. Chem. Res.*, 55 (2016) 11878
24. Y. Melamed, N. Maity, L. Meshi and N. Eliaz, *Coatings*, 11 (2021) 1414
25. J. P. M. Veder, M. D. Horne, T. Rütger, A. M. Bond and T. Rodopoulos, *Electrochem. Commun.*, 37 (2013) 68
26. S. Z. E. Abedin, E. M. Moustafa, R. Hempelmann, H. Natter and F. Endres, *ChemPhysChem*, 7 (2006) 1535
27. X. Sun, Y. Fang, X. Jiang, K. Yoshii, T. Tsuda and S. Dai, *Chem. Commun.*, 52 (2016) 292
28. A. Bakkar and V. Neubert, *Electrochem. Commun.*, 51 (2015) 113
29. T. Rodopoulos, L. Smith, M. D. Horne and T. Rütger, *Chem. Eur. J.*, 16 (2010) 3815
30. P. Eiden, Q. Liu, S. Z. E. Abedin, F. Endres and I. Krossing, *Chem. Eur. J.*, 15 (2009) 3426
31. O. M. Leung, T. Schoetz, T. Prodromakis and C. P. D. Leon, *J. Electrochem. Soc.*, 168 (2021) 056509
32. Y. Zheng, C. Peng, Y. Zheng, D. Tian and Y. Zuo, *Int. J. Electrochem. Sci.*, 11 (2016) 6095
33. M. Zhang, J. S. Watson, R. M. Counce, P. C. Trulove and T. A. Zawodzinski, *J. Electrochem. Soc.*, 161 (2014) D163
34. X. Tu, J. Zhang, M. Zhang, Y. Cai, H. Lang, G. Tian and Y. Wang, *RSC Adv.*, 7 (2017) 14790
35. G. Yue, X. Lu, Y. Zhu, X. Zhang and S. Zhang, *Chem. Eng. J.*, 147 (2009) 79
36. S. Z. E. Abedin, P. Giridhar, P. Schwab and F. Endres, *Electrochem. Commun.*, 12 (2010) 1084

37. Y. Zheng, S. Zhang, X. Lu, Q. Wang, Y. Zuo and L. Liu, *Chin. J. Chem. Eng.*, 20 (2012) 130

© 2022 The Authors. Published by ESG (www.electrochemsci.org). This article is an open access article distributed under the terms and conditions of the Creative Commons Attribution license (<http://creativecommons.org/licenses/by/4.0/>).